International Journal of
Plant Biology

MDPI

Article

Adaptability, Yield Stability, and Agronomic Performance of Improved Purple Corn (*Zea mays* L.) Hybrids Across Diverse Agro-Ecological Zones in Peru

Gilberto Garcia [1], Fernando Montero [1], Maria Elena Torres [2], Selwyn Alvarez [2], Wildo Vasquez [3], Abraham Villantoy [3], Yoel Ruiz [4], Fernando Escobal [4], Hector Cántaro-Segura [5], Omar Paitamala [6] and Daniel Matsusaka [6,*]

1 Estación Experimental Agraria Vista Florida, Dirección de Supervisión y Monitoreo de las Estaciones Experimentales, Instituto Nacional de Innovación Agraria (INIA), Chiclayo 14300, Peru
2 Estación Experimental Agraria Arequipa, Dirección de Supervisión y Monitoreo de las Estaciones Experimentales, Instituto Nacional de Innovación Agraria (INIA), Arequipa 04001, Peru
3 Estación Experimental Agraria Chumbibamba, Dirección de Supervisión y Monitoreo de las Estaciones Experimentales, Instituto Nacional de Innovación Agraria (INIA), Apurimac 08001, Peru
4 Estación Experimental Agraria Baños del Inca, Dirección de Supervisión y Monitoreo de las Estaciones Experimentales, Instituto Nacional de Innovación Agraria (INIA), Cajamarca 06001, Peru
5 Centro Experimental La Molina, Dirección de Recursos Genéticos y Biotecnología, Instituto Nacional de Innovación Agraria (INIA), Lima 15200, Peru
6 Dirección de Investigación y Desarrollo Tecnológico (DIDET), Instittuto Nacional de Innovación Agraria (INIA), Av La Molina 1981, Lima 15200, Peru
* Correspondence: dmatsusaka@agro.uba.ar

Abstract

Purple corn (*Zea mays* L.) is a nutraceutical crop of increasing economic importance in Peru, yet its productivity is highly influenced by genotype × environment (G × E) interactions across heterogeneous agro-ecological zones. Therefore, selecting suitable genotypes for specific environments is essential to optimize variety deployment and maximize site-specific yield. Five purple-maize genotypes (INIA-601, INIA-615, Canteño, PMV-581, and Sintético-MM) were evaluated in four contrasting Peruvian sites using a randomized complete-block design. Grain yield, field weight, anthesis–silking interval (ASI), plant height, and ear-rot incidence were analyzed with combined analysis of variance (ANOVA), the additive main effects and multiplicative interaction (AMMI), genotype and genotype-by-environment (GGE) biplots, Weighted Average of Absolute Scores (WAAS), weighted average of absolute scores and best yield index (WAASBY), and Y × WAAS indices. Environment accounted for 90.1% of field-weight variation ($p < 0.0001$) and 50.2% of grain-yield variation ($p < 0.001$), while significant G × E interactions (3.93% and 18.14%, respectively) justified bilinear modeling. AMMI1 and GGE "which-won-where" biplots identified INIA-615 and PMV-581 as broadly adapted, with INIA-615 achieving the highest WAASBY and positioning in quadrant IV of Y × WAAS (high yield, high stability). INIA-601 and Sintético-MM exhibited exceptional stability (low ASV) but moderate productivity; Canteño showed limited adaptability. Chumbibamba emerged as a key discriminating, high-productivity location. From an agronomic perspective, INIA-615 is recommended for high-productivity valleys such as Sulluscocha and Santa Rita, where its yield potential and stability are maximized. These findings underscore the potential of integrating multivariate stability metrics with physiological and disease-resistance traits to guide the selection of superior purple corn cultivars. Overall, INIA-615 represents a robust candidate for enhancing yield stability, supporting sustainable intensification, and expanding the nutraceutical value chain of purple corn in the Andean highlands.

Academic Editor: Adriano Sofo

Received: 16 October 2025
Revised: 18 November 2025
Accepted: 19 November 2025
Published: 25 December 2025

Keywords: purple corn; genotype × environment interaction; AMMI and GGE biplot; yield stability; multi-environmental trials

1. Introduction

Peru harbors an exceptional level of natural genetic diversity, which has enabled the domestication and diversification of a wide range of crops. Among these, purple corn (*Zea mays* L.) stands out as one of the 52 landraces classified within the Kculli race, traditionally cultivated in the Andean highlands [1]. Its intense purple pigmentation is due to the accumulation of anthocyanins, a subclass of flavonoids localized in the bracts, kernels, and cob, which exhibit effective antioxidant properties [2,3].

Notably, anthocyanins in purple corn have demonstrated superior free radical scavenging activity compared to other common antioxidants such as quercetin [4], catechins [5], and butylated hydroxyanisole [6]. These properties have contributed to the growing recognition of purple corn as a nutraceutical crop with potential health benefits, including mitigating oxidative stress and reducing the risk of cardiovascular diseases and certain cancers [7,8]. As a result, market demand has increased significantly, and its production in Peru has shown sustained growth over the past five years, with the national average yield reaching [9].

Agronomic performance in maize frequently exhibits significant differences when grown across diverse environments [10]. In particular, grain yield and quality in maize are highly influenced by both genetic and environmental factors, making it essential to investigate genotype × environment (G × E) interactions to identify cultivars with high adaptability and phenotypic stability across diverse agro-ecological zones [11–14]. Therefore, G × E interactions provide insights for identifying genotypes that combine superior average performance with stability under variable field conditions [15,16]. This evaluation aimed to identify and distinguish genotypes that combine superior average performance with robust stability across a range of environmental conditions, which is indispensable for selecting cultivars that exhibit both high productivity and adaptability in multi-environment trials [17].

Furthermore, modern hybrid development focuses on achieving both high and stable yields across a broad spectrum of environmental conditions. The successful identification of such hybrids depends on rigorous evaluation under diverse environmental scenarios [18]. However, their adaptation is a gradual and long-term process, necessitating extensive multi-location trials before they can be confidently recommended for specific agro-ecological zones [19,20]. As highlighted by Yan et al. [21], genotype performance in multi-environment trials is significantly influenced not only by the main effects of genotype (G) and environment (E), but also by their interaction (G × E), which often plays a decisive role in determining yield outcomes.

The urgency of resolving G × E complexities is amplified by climate change and the rising demand for nutritionally rich crops like purple corn. Recent advances in G × E analysis, particularly using the additive main effects and multiplicative interaction (AMMI) model, offer an effective framework to dissect G × E interactions and identify genotypes that consistently perform well across variable environments [22–27]. These approaches have been increasingly applied in Andean crops, including purple corn, due to their ability to decompose interaction effects and inform breeding strategies under climatic uncertainty [2,28].

In this evolving context, robust statistical tools are essential to identify adaptive responses and environmental suitability. AMMI models offer a powerful framework to

elucidate adaptation patterns in complex environments, enabling more precise genotype selection [29,30]. Furthermore, complementary indices such as the AMMI Stability Value (ASV), Weighted Average of Absolute Scores (WAAS), and WAASBY provide integrative assessments of genotype performance and stability [31,32]. Meanwhile, GGE biplot analysis has emerged as a standard method for visually interpreting "which-won-where" patterns, facilitating the identification of mega-environments and specifically adapted genotypes [33].

This evaluation is particularly relevant in the Peruvian Andes, where heterogeneous agro-ecological conditions pose a challenge for stable and high-performing cultivar deployment. The objective of this study was to evaluate the agronomic performance and stability of five purple corn genotypes (INIA-601, INIA-615 Negro Canaán, Canteño, PMV-581, and Sintético-MM) across four contrasting regions of Peru: Arequipa, Ayacucho, Cajamarca, and La Libertad. By applying the additive main effects and multiplicative interaction (AMMI) model more tightly with complementary stability indices, including genotype and genotype-by-environment (GGE) biplots, Weighted Average of Absolute Scores (WAAS), weighted average of absolute scores and best yield index (WAASBY), and Y × WAAS indices. This study aimed to assess the adaptability and phenotypic stability of purple corn genotypes using a combination of multivariate stability models. The objective was to identify those genotypes exhibiting superior yield stability and adaptability across distinct agro-ecological zones of Peru. The findings are expected to provide valuable insights for breeding programs and to support the sustainable intensification and geographical expansion of purple corn cultivation within highland agroecosystems

2. Materials and Methods

2.1. Study Site

The field experiment was conducted during the 2023–2024 cropping season across four contrasting agro-ecological zones in Peru: (i) Sulluscocha, Namora district, Cajamarca (78°22′38.32″ W, 07°12′16.25″ S, 2987 m.a.s.l.), with a maximum temperature of 25.7 °C, minimum of 3 °C, average of 16.5 °C, and 61.2% relative humidity. (ii) Vista Florida Experimental Station, Pisci district, Lambayeque (79°46′49″ W, 06°43′44″ S, 42 m.a.s.l.), with temperatures ranging from 11.8 °C to 30.0 °C and 75% relative humidity. (iii) Santa Rita de Siguas, Arequipa (72°05′22″ W, 16°29′35″ S, 1265 m.a.s.l.), with an average temperature of 19.8 °C, maximum of 33.9 °C, minimum of 5.2 °C, and 52.1% relative humidity. (iv) Chumbibamba, Apurímac (73°23′18″ W, 13°39′02″ S, 2890 m.a.s.l.), with temperatures ranging from 10.3 °C to 13.5 °C and 78.2% relative humidity (Figures 1 and 2).

Before establishing the trial, composite soil samples (15 subsamples per site, 0–30 cm depth) were collected, homogenized, and analyzed in the soil, water, and foliar laboratories (LABSAF) of each experimental station. The soils displayed substantial heterogeneity across environments (Table 1).

Table 1. Soil chemical properties at the experimental sites prior to the implementation of management practices.

Physicochemical Properties	Units	Environment			
		Vista Florida	Santa Rita	Chumbibamba	Sulluscocha
pH	unid. pH	7.7	7.7	6.5	8.1
Electrical conductivity	mS/m	3.1	117.4	3.6	11.5
Organic matter	%	1.25	1.4	2.5	4.0
Nitrogen	%	-	-	0.13	-
Available phosphorus	mg/kg	6.6	69.5	57.8	13.9
Available potassium	mg/kg	128	813.38	146.38	277.1
Calcium carbonate equivalent	%	3.06	2.1	-	12.69

Table 1. *Cont.*

Physicochemical Properties	Units	Environment			
		Vista Florida	Santa Rita	Chumbibamba	Sulluscocha
		SoilTexture			
Sand	%	60	78.6	48	-
Silt	%	17	10.2	22	-
Clay	%	23	11.2	30	-
Textural Class		Sandy clay loam	Loam	Clay loam	Clay loam

Note: "-" indicates that no data were available.

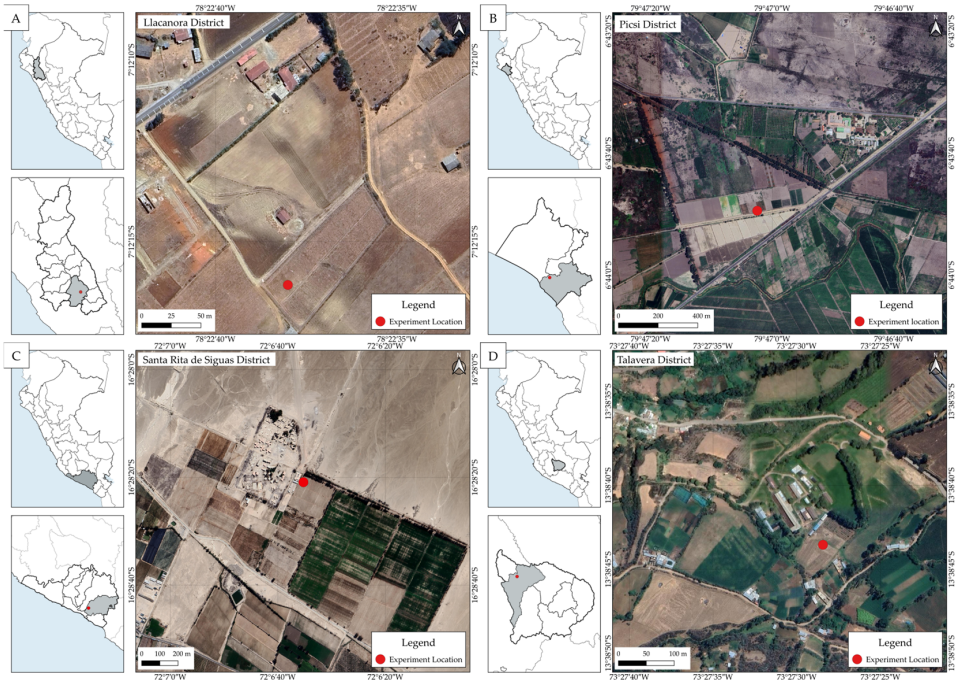

Figure 1. Experimental trials were conducted in four locations across different agro-ecological regions of Peru. The gray-shaded area in each inset map represents the department where the experiment was carried out, and the red dots indicates the specific location within the province. (**A**) Sulluscocha (Cajamarca), (**B**) Vista Florida (Lambayeque), (**C**) Santa Rita de Siguas (Arequipa), and (**D**) Chumbibamba (Apurímac).

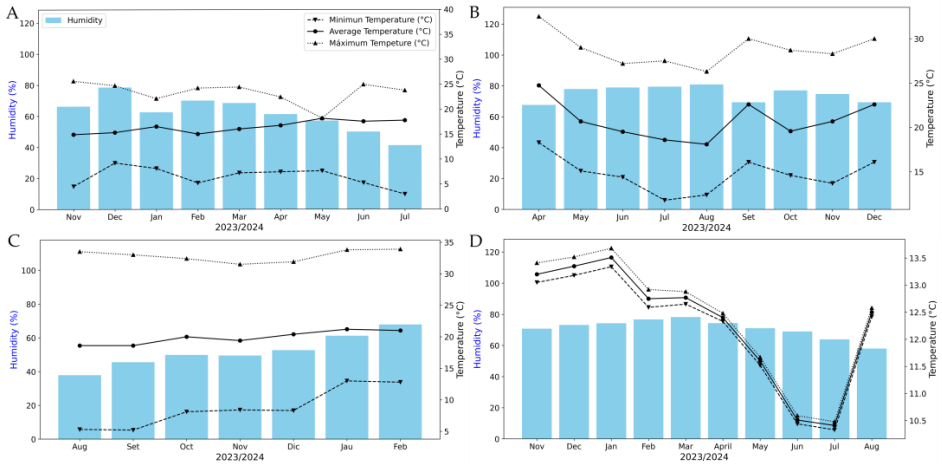

Figure 2. Temperature and humidity recorded during the experimental period. (**A**) Sulluscocha, (**B**) Vista Florida, (**C**) Santa Rita Experimental Station, and (**D**) Chumbibamba Experimental Station.

2.2. Plant Material and Treatments

Five purple corn genotypes with high yield potential and agronomic adaptability were evaluated: Canteño (G1), INIA-601 (G2), INIA-615 (G3), PMV-581 (G4), and Sintético-MM (G5) hybrids (Table 2).

Table 2. Genetic origin and key agronomic traits of the five purple corn genotypes evaluated across four Peruvian environments.

Genotype	Description	Reference
INIA 601	This variety was developed in 1990 at the Cajabamba Experimental Station. It originated from a population of 256 progenies, comprising 108 derived from the purple corn variety *Caraz* and 148 from the local variety *Negro Bañosbamba*. INIA-601 is characterized by a plant height of 2.16 m, female flowering at 98 days, a thousand-seed weight of 456.2 g, and an average grain yield of 3.0 t ha^{-1}.	[34]
INIA 615	Developed from 36 collections of Kully-race local cultivars gathered in 1990 from the provinces of Huanta, Huamanga, and San Miguel, this variety was refined through nine consecutive cycles of half-sib recurrent selection. It was improved through nine cycles of half-sib recurrent selection. INIA-615 exhibits the following characteristics: plant height of 2.28 m, female flowering between 84 and 92 days, and an average commercial yield of 7.8 t ha^{-1}.	[35]
Canteño	Derived from the Cuzco race, this variety represents the predominant purple corn consumed in Lima. It is characterized by large kernels arranged in well-defined rows on the cob. The Canteño variety shows an average grain yield ranging from 1.50 to 1.90 t ha^{-1}.	[2,36,37]
PMV 581	PMV-581 is an improved purple corn genotype developed at the Universidad Nacional Agraria La Molina using germplasm derived from Morado de Caraz. It has an intermediate growth cycle and produces elongated, medium-sized ears (15–20 cm) with high anthocyanin content. Under well-managed production conditions, PMV-581 can reach grain yields of up to 6 t ha^{-1}.	[38]
Sintético-MM	Morado Mejorado (MM) is a synthetic purple corn variety derived from INIA 601 and developed through recurrent selection of S1 progenies at the Baños del Inca Experimental Station (INIA–Peru).	[2]

2.3. Experimental Design and Agronomic Management

A randomized complete-block design (RCBD) was implemented with three replications and five genotypes randomly distributed within each block. Each experimental unit measured 16 m^2 (5.00 m length × 3.20 m width), consisting of four rows spaced 0.75 m apart. Plants were spaced at 0.50 m within rows, with 10–12 planting spots per row, with two to three seeds sown per hill. This arrangement resulted in an effective planting density of approximately 7 plants m^{-2}. The seeds were placed at a depth approximately twice their size (about 4–5 cm). Buffer zones of 1.00 m between blocks and 0.80 m at plot ends were maintained to minimize border effects (Figure S1).

Field preparation was conducted one month before sowing through mechanical tillage, including plowing, harrowing, and leveling. Irrigation and fertilization practices varied among locations depending on soil fertility and available technology. Fertilization was adjusted according to soil analysis and local recommendations, applying mineral fertilizers equivalent to 180–80–60 (Santa Rita), 240–120–140 (Vista Florida), 90–120–60 (Sulluscocha), and 120–90–60 kg ha^{-1} (Chumbibamba) of N–P_2O_5–K_2O. The nitrogen source was urea (46% N), phosphorus was supplied as monoammonium phosphate (MAP, 11–52–0), and potassium as potassium chloride (KCl, 60% K_2O), split between sowing and hilling.

Two hilling operations were performed, the first when plants reached 30 cm in height and the second between 40 and 50 cm to improve root anchorage, aeration, and weed

suppression. Weed control was conducted manually during the first 45 days after sowing, and subsequent weeding was carried out before flowering and during grain filling to prevent competition. Irrigation frequency was adjusted according to phenological stages. Deep irrigation was applied during crop establishment, followed by regular irrigation during vegetative growth. A drip irrigation system was used exclusively to maintain optimal soil moisture throughout the cycle; no water deficit or drought-stress conditions were imposed at any location. Soil moisture was kept stable during flowering and grain filling to avoid water stress, which could otherwise affect reproductive traits such as the anthesis–silking interval (ASI).

Phytosanitary management followed local agricultural guidelines. For *Spodoptera frugiperda*, targeted applications of Spinetoram and Chlorantraniliprole (10 mL per 20 L of water) were used. For *Helicoverpa zea*, three drops of vegetable oil were applied on the silk tips of each ear. Preventive fungicide and systemic insecticide treatments were applied only when pest incidence exceeded 10%.

2.4. Agronomic Traits Measured

Male flowering (days): Number of days from sowing until 50% of plants exhibited tassels; and Female flowering (days): Number of days from sowing to 50% silking. The anthesis–silking interval (ASI) was obtained from the time gap between male and female flowering days. Plant height (cm): Measured on ten randomly selected plants per plot, from ground level to the tip of the tassel, recorded approximately one week before harvest. Cob rot incidence (%): Proportion of ears showing visible rot symptoms over the total number evaluated per plot. Field weight was obtained by harvesting the two central rows of each plot when the grain moisture content was approximately 20–25%.

Grain moisture (%): At harvest, grain moisture was measured in each experimental unit to obtain the actual %H used for yield correction. In all locations, ten ears were randomly selected per plot; two central rows of each ear were shelled, and grain samples were analyzed using a DRAMINSKI grain moisture and weight meter (model: GMDM). The measured %H values were incorporated into the grain-yield correction to the standard 14% moisture basis.

Grain yield (t/ha): Estimated using the formula:

$$\text{GY (t/ha)} = \text{PC} \times (10/\text{AEP} \times (100 - \%\text{H})/86) \times \text{ID}$$

where GY = grain yield (t/ha), PC = field weight (kg), H = grain moisture (%), 86 = standard correction factor for 14% moisture, and ID = harvest index (0.8).

In this study, grain yield was calculated using a fixed harvest index of 0.8, representing the threshing coefficient, defined as the proportion of grain relative to total ear weight. Kernels were manually separated from the cob using a hand sheller, and routine field measurements in purple corn confirm that grain-to-ear ratios typically approximate 0.8 under standard agronomic conditions.

Field weight, grain yield, and cob-rot incidence were all determined after harvest.

2.5. Statistical Analysis

The data were subjected to combined analysis of variance (ANOVA) to determine the significance of main effects and genotype × environment (G × E) interactions. The AMMI (Additive Main Effects and Multiplicative Interaction) model was used to partition G × E interaction into principal components and to explore the interaction structure [22–27,29]. Stability was assessed using the AMMI Stability Value (ASV) and WAAS (Weighted Average of Absolute Scores) index [30,31]. The WAASBY index was

calculated to integrate mean performance and stability. GGE biplots were used to visualize the "which-won-where" pattern of genotype performance across environments [31]. All statistical analyses were performed in R software (version 4.5.0), using the metan package (version 1.19.0) [32].

3. Results

3.1. Plant Height (cm)

The analysis of the additive main effects and multiplicative interaction (AMMI) analysis revealed that the environment (ENV) was the main contributor to the total variation in plant height, explaining 90.80% of the total sum of squares, and showed a highly significant effect (F = 310.74, p = 0.0001). The genotype (GEN) effect was also a statistically significant effect (F = 5.58, p = 0.001577), although it contributed a smaller portion of the variance (2.85%). In contrast, the genotype × environment interaction (G × E) was not significant (F = 0.96, p = 0.503) and accounted for 1.47% of the total variation, indicating that genotypes responded similarly across environments (Table S1)

The contribution of the first principal component axis (PC1) explained 66.8% of the G × E interaction, and its associated F-value was not significant (F = 1.28, p = 0.294), confirming the lack of structured interaction patterns. While the second principal component axis, PC2, accounted for 30.1%, both together captured 96.9% of the interaction sum of squares (Table S1).

Additionally, the GGE biplot (Which-won-where) was included for exploratory purposes. While typically applied under significant G × E conditions, it offered a visual interpretation of the distribution of genotypes across environments. The polygon connecting the vertex genotypes (G1, G3, G4, and G5) delineates the mega-environments. Santa Rita, located in the upper-right quadrant, is clearly associated with G4 (238.91 ± 14.90 cm), indicating superior performance but a more specific adaptation. Conversely, Vista Florida, Chumbibamba, and Sulluscocha cluster in the lower-right quadrant, where G5 (243.96 ± 13.27 cm) exhibits the highest performance and broader adaptability across these environments. G2 (239.17 ± 12.89 cm), positioned near the origin, reflects average performance and greater stability but lacks specific superiority in any environment. In contrast, G1 (223.93 ± 13.03 cm) and G3 (226.67 ± 14.35 cm), located on the left side of the plot, exhibit poor performance and limited adaptation. Overall, these results highlight G4 as a promising candidate for targeted environments such as Santa Rita, while G5 demonstrates versatility and adaptability, making it suitable for broader deployment across diverse production conditions (Figure 3).

Despite the non-significant interaction, the AMMI Stability Value (ASV) plot provided exploratory insights: genotype G5 (1.25) had the lowest ASV and one of the highest plant heights (243.96 cm). Conversely, G2 (3.15), G4 (3.21), and G1 (3.51) displayed higher ASV scores and moderate plant height, indicating less stability (Figure S2).

3.2. Anthesis–Silking Interval (ASI)

The AMMI analysis for the anthesis–silking interval (ASI) revealed that the environment (ENV) explained 53.68% of the total variance and was highly significant (F = 36.38, p = 0.0001), indicating a strong environmental effect on ASI (Table S2). The genotype effect (F = 1.68, p = 0.1771) and genotype × environment interaction (F = 0.81, p = 0.6341) were not statistically significant. Despite this, both principal components explained 97.01 of the G × E interaction, although it was not statistically significant (p = 0.3124), reinforcing the absence of meaningful crossover interaction (Table S2).

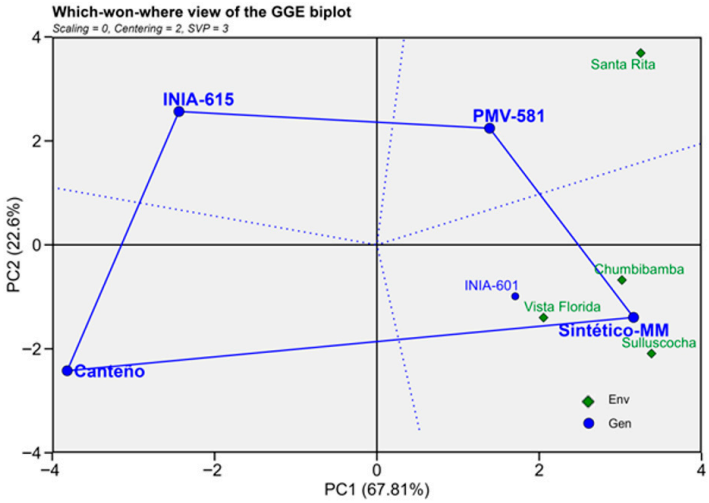

Figure 3. Which-won-where view of the GGE biplot for plant height (cm) displaying the scores of principal component 2 (PC2) versus principal component 1 (PC1) across four environments for five maize genotypes. The solid blue lines represent the convex polygon connecting the most responsive genotypes, while the dotted blue lines divide the biplot into sectors used to identify the winning genotype in each environment.

The GGE biplot was used to explore patterns of genotypic adaptation and explained 87.41% of the total variation. The vertex genotypes (G1–G5) define the interaction patterns and help identify mega-environments. G2 (5.29 ± 0.35 days), located in the upper-right quadrant and closest to Sulluscocha, exhibited the most favorable ASI response in that environment, indicating a better synchronization of male and female flowering under those conditions. G3 (5.93 ± 0.80 days), with the highest ASI, showed superior performance in Vista Florida and moderate adaptation to Chumbibamba and Santa Rita, while G5 (5.10 days), positioned on the opposite side of the biplot, displayed poor adaptation across all environments. Meanwhile, G1 (4.52 ± 0.60 days) and G4 (4.43 ± 0.48 days), grouped near the origin, demonstrated more stable ASI performance, although they lacked clear dominance in any environment. These results indicate that G2 and G3 possess potential for targeted improvement of flowering synchrony in highland environments such as Sulluscocha and Vista Florida, respectively (Figure 4).

The ASV plot showed that G4 (0.58) and G3 (0.64) were the most stable genotypes, presenting the lowest ASV values along with the shortest ASI (≤6 days), which is agronomically desirable under stress conditions. Conversely, G5 (1.14), G2 (1.27), and G1 (1.46) displayed higher ASV values and longer ASI durations (Figure S3).

3.3. Cob Rot (%)

The AMMI analysis for cob-rot incidence (%) showed that the environmental effect (ENV) was highly significant ($F = 679.41$, $p = 0.0001$) and accounted for 97% of the total variation. Conversely, the genotypic ($F = 1.50$, $p = 0.2255$) effect and the genotype × environment interaction ($F = 0.99$, $p = 0.478$) were not significant. The proportion of variance attributed to PC1 (65.6%) and PC2 (31.8%) further confirms that while the interaction exists, it is not structured enough to be significant. (Table S3).

Although the G × E term was not significant, a GGE 'which-won-where' biplot (PC1 = 70.57%, PC2 = 25.47%) was constructed to visualize genotype behavior across environments, explaining 97.1% of the total variation. The polygon formed by the vertex genotypes (G2, G3, G4, and G5) delineates interaction patterns and identifies distinct mega-environments. In this context, the vertex genotype within each sector represents the least

resistant entry, in other words, the one exhibiting the highest cob-rot incidence under the environmental configuration defined by that sector. G3 (18.50 ± 6.12%), located at the upper vertex, is strongly associated with Chumbibamba, revealing a higher susceptibility to cob rot in these environments. Conversely, G4 (17.20 ± 5.46%), situated in the right quadrant, demonstrated a more favorable performance, indicating lower cob-rot incidence in those environments. G5 (19.78 ± 6.04%), positioned near the lower center, exhibits moderate to high susceptibility, particularly in Santa Rita, while G2 (20.34 ± 6.66%), in the left quadrant, shows intermediate performance with some adaptation to Vista Florida and Sulluscocha locations. Genotypes located near the origin, such as G1 (19.82 ± 6.03%), displayed greater stability across environments but did not excel in resistance. These findings highlight G4 as a promising genotype for reducing cob-rot incidence under diverse conditions, while G3 requires targeted management in environments where disease pressure is higher (Figure 5).

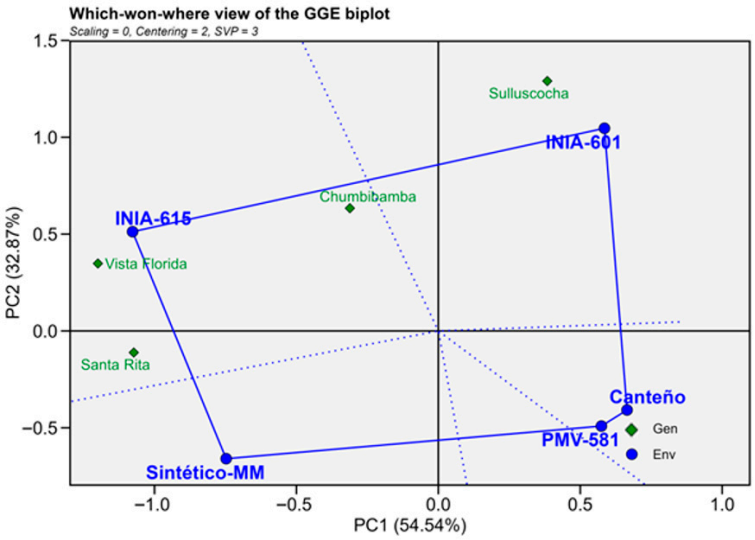

Figure 4. Which-won-where view of the GGE biplot for ASI across four environments. The solid blue lines represent the convex polygon connecting the most responsive genotypes, while the dotted blue lines divide the biplot into sectors used to identify the winning genotype in each environment.

In the ASV plot, G1 (0.56) and G5 (0.79) exhibited the lowest ASV values and moderate cob-rot levels, indicating greater phenotypic stability. In contrast, the elevated ASV scores observed in G2 (1.72), G4 (1.74), and G3 (2.08) reflect reduced stability across environments (Figure S4).

For plant height, Anthesis–Silking Interval (ASI), and cob-rot percentage, no significant G × E interaction was detected, indicating a consistent genotypic response across environments. In contrast, both yield-related traits exhibited significant interactions across environments. Consequently, a more detailed AMMI analysis was conducted for the yield components to capture the complexity of these significant interactions and to better understand the stability and adaptability patterns among genotypes under varying agro-ecological conditions.

3.4. Field Weight (kg)

The analysis of variance (ANOVA) for field weight (kg) revealed that the environmental effect was the primary contributor to phenotypic variation, accounting for 90.1% of the total variation, which was statistically significant ($F = 324.69$, $p < 0.0001$). However, the genotype factor was not statistically significant ($F = 1.48$, $p < 0.02$). The genotype × environment interaction (G × E) was also significant ($F = 2.37$, $p = 0.02$), accounting for 3.93% of the total variation, justifying the use of the AMMI model for further exploration of G × E patterns.

In contrast, the genotypic (GEN) effect was not significant, explaining only 0.82% of the total variation (Table S4).

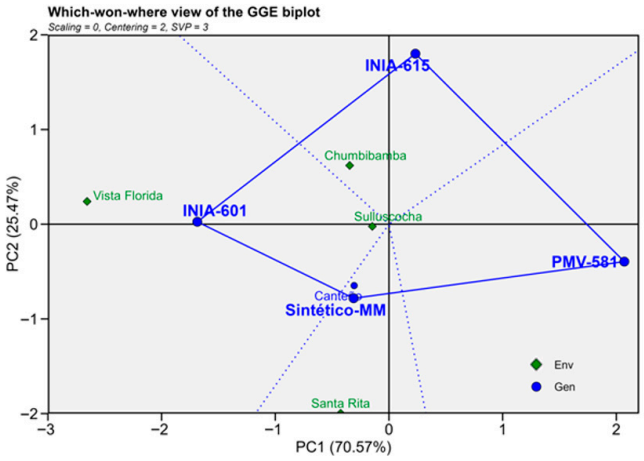

Figure 5. Which-won-where view of the GGE biplot for cob-rot incidence (%) across four environments. The solid blue lines represent the convex polygon connecting the most responsive genotypes, while the dotted blue lines divide the biplot into sectors used to identify the winning genotype in each environment.

Supporting this, the AMMI1 biplot clearly distinguished the interaction patterns among genotypes and environments. G2 (0.99), G3 (0.51), and G5 (0.54) showed positive PC1 scores and were located near the origin of the interaction axis, denoting superior phenotypic stability and broad adaptability across environments. In contrast, G4 (−0.51) and G1 (−1.53) exhibited negative PC1 scores, indicating greater interaction with specific environments and reduced stability. Among environments, Chumbibamba (16.3 ± 0.22 kg) showed the highest mean performance but also strong interaction effects (negative PC1), whereas Sulluscocha (4.86 ± 0.28 kg) and Santa Rita (7.96 ± 0.61 kg) were more associated with genotypes showing positive PC1 values and higher overall stability (Figure 6).

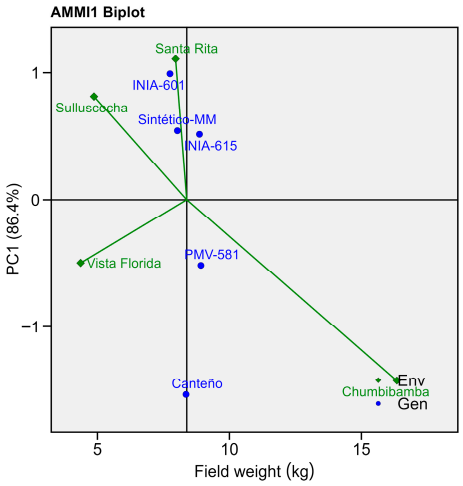

Figure 6. AMMI1 biplot for field weight (kg), illustrating the genotype × environment interaction. The x-axis represents the mean field weight, while the y-axis corresponds to the first principal component (PC1), which explains 86.4% of the interaction sum of squares. The green lines represent the environment vectors, indicating the direction and magnitude of the environmental effects on the G×E interaction.

The GGE biplot "which-won-where" illustrates the interaction between genotypes and environments for field weight (kg). The biplot is based on PC1 and PC2, which together

explain 89.39% of the total variation. The polygon highlights the genotypes with the greatest interaction effects, forming four sectors. G3 (8.86 ± 1.48 kg) was the winning genotype in Santa Rita and Sulluscocha, while G4 (8.92 ± 1.50 kg) performed best in Vista Florida and Chumbibamba. Whereas G1 (8.35 ± 1.83 kg) and G2 (7.74 ± 2.76 kg) were not associated with any specific environment. In contrast, G5 (8.02 ± 1.43 kg) was positioned near the origin, indicating greater phenotypic stability across environments. (Figure 7).

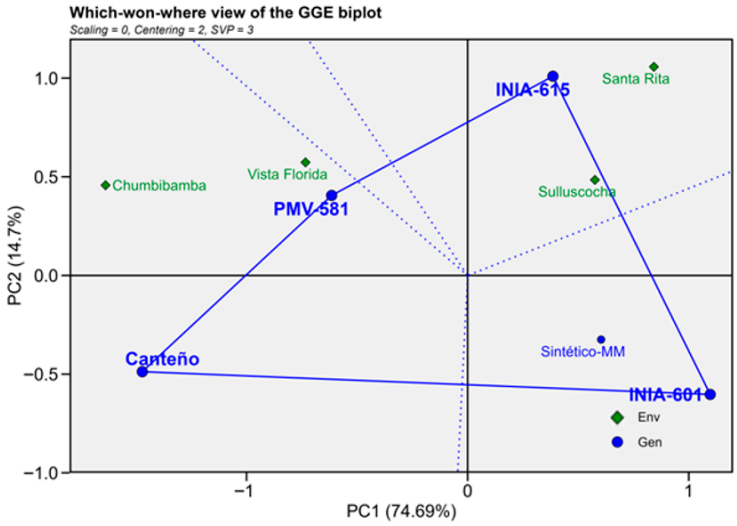

Figure 7. Which-won-where view of the GGE biplot for field weight (kg). The polygon connects the genotypes farthest from the biplot origin, with sectors indicating which genotype performed best in each environment. The solid blue lines represent the convex polygon connecting the most responsive genotypes, while the dotted blue lines divide the biplot into sectors used to identify the winning genotype in each environment.

The ASV (AMMI Stability Value) plot showed that G5 (0.68) and G2 (1.37) displayed the lowest ASV values, indicating higher stability. These genotypes showed moderate to low field-weight values. Conversely, G1 (1.65), G3 (1.72), and G4 (1.88) combined good performance with slightly higher ASV scores, indicating an intermediate balance between stability and productivity (Figure S5)

In the WAASBY plot, G4 (99.97%) and G3 (97.68%) achieved the highest indices, reinforcing their superior performance and stability across test environments. In contrast, G1 (25.96%) and G2 (26.65%) had below-average WAASBY values (red), confirming their limited adaptability and lower yield efficiency under variable conditions (Figure 8).

Finally, the Y × WAAS biplot provides a joint assessment of field weight (kg) and stability of the genotypes across environments, effectively summarizing the genotype × environment (G × E) interaction. Genotypes G4 and G5, positioned in the fourth quadrant (high yield–high stability), demonstrated consistent performance across environments, with G3 exhibiting slightly superior stability. Conversely, G1 and G2, located in the first quadrant, showed low yield combined with greater instability, making them less desirable for broad adaptation. Among environments, Chumbibamba was identified as the most productive location, while Vista Florida and Sulluscocha favored genotypes with more stable responses, underscoring their potential suitability for environments with lower stress variability (Figure 9).

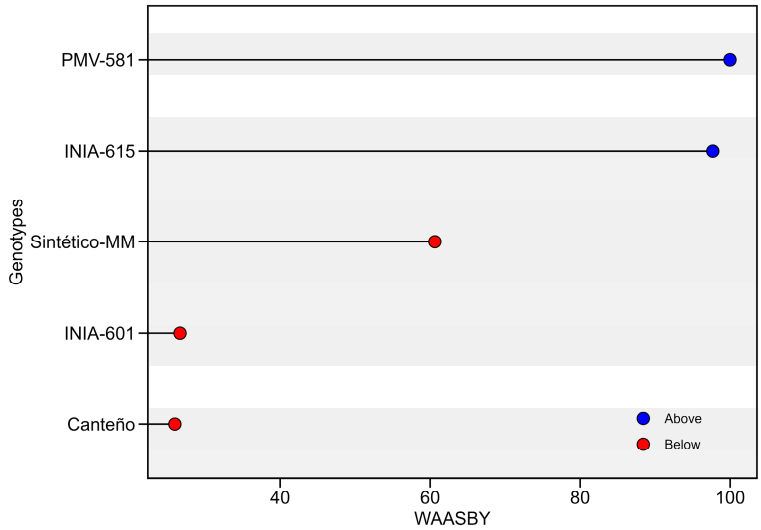

Figure 8. WAASBY index for genotype ranking based on yield (kg) and stability. The horizontal axis reports the WAASBY value, an integrated measure in which higher scores denote a more desirable combination of grain-yield performance and stability, while the vertical axis lists genotypes in descending order of WAASBY. WAASBY values, expressed on a 0–100% scale. Points are color-coded relative to the overall WAASBY mean (blue = above-average; red = below-average).

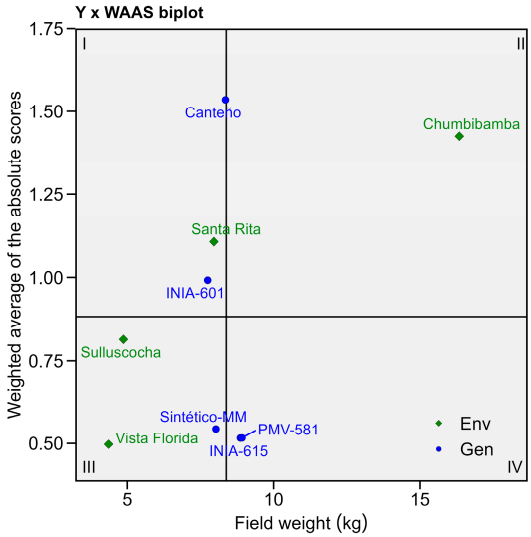

Figure 9. Y × WAAS biplot for field weight (kg), classifying genotypes and environments into four quadrants. The horizontal axis represents the mean field weight, while the vertical axis reflects the weighted average of the absolute scores (WAAS), where lower values indicate greater stability.

3.5. Grain Yield (t/ha)

The AMMI analysis of variance revealed a highly significant effect of environment on grain yield (F = 39.25, p = 0.001), while the genotypic effect was not significant (F = 1.57, p = 0.204), and the genotype-by-environment (G × E) interaction was marginally significant (F = 2.05, p = 0.052). Although the environments differed markedly in altitude, temperature, and soil fertility, the G × E interaction remained weak because the evaluated genotypes exhibited similar response patterns across environments, with no strong crossover interactions.

The environment explained the largest proportion of the total variance (50.20%), followed by the G × E interaction (18.14%), underscoring the importance of environmental influence and specific G × E patterns on genotype performance. These results justify the

use of bilinear models such as AMMI and GGE biplots to evaluate the adaptability and stability of the evaluated purple corn genotypes (Table S5).

The AMMI1 biplot accounted for 84.3% of the total G × E interaction. Genotypes G3 (5.2 ± 0.44 t/ha) and G2 (4.50 ± 0.37 t/ha) maintained high mean grain yield and relatively low interaction scores (PCA1), positioning them as promising candidates for broad adaptability. In contrast, G1 (4.65 ± 0.51 t/ha) and G4 (5.16 ± 0.50 t/ha) showed greater interaction effects, indicating specific adaptability. Among environments, Santa Rita (5.62 ± 0.42 t/ha) and Sulluscocha (2.96 ± 0.21 t/ha) were the most discriminating, while Vista Florida (5.42 ± 0.37 t/ha) and Chumbibamba (5.17 ± 0.18 t/ha) contributed less to genotype differentiation (Figure 10).

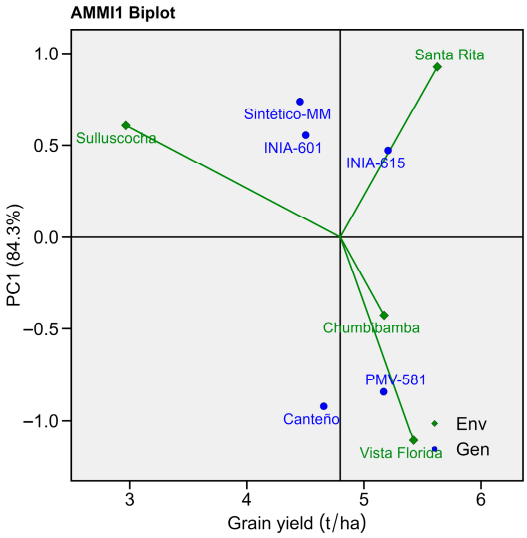

Figure 10. AMMI1 biplot for grain yield (t/ha) across environments. The green lines represent the environment vectors, indicating the direction and magnitude of the environmental effects on the G×E interaction.

To complement the AMMI analysis, the GGE 'which-won-where' biplot (SVP = 3) explained 93.94% of the total variation, with PC1 and PC2 accounting for 70.43% and 23.51%, respectively. Genotypes G1, G3, G4, and G5 were located at the vertices of the polygon, indicating superior performance in specific environments: Chumbibamba, Vista Florida, and Sulluscocha–Santa Rita for G1, G4, and G3, respectively. G2 was near the origin, reflecting broad adaptability and low interaction with the environment (Figure 11).

To evaluate yield stability explicitly, the ASV (AMMI Stability Value) versus grain yield plot was applied. G3 stood out with the highest yield and lowest ASV (0.76), indicating an excellent balance between productivity and stability. G4 (1.50) showed a competitive yield but a higher ASV, reflecting greater interaction with specific environments. G1 (1.62) and G5 (1.20) showed high ASV and moderate to low yields, making them less suitable for general recommendation (Figure S6).

The WAASBY index efficiently combined mean performance and stability to identify the most desirable genotypes across environments. In this analysis, G3 exhibited the highest WAASBY value of 100, highlighting its superior adaptability and consistent yield performance across test locations. Similarly, G4 (56.22%) also showed a favorable balance between yield potential and stability, positioning it as a promising candidate for broader cultivation. In contrast, G1 (13.51%) and G5 (20.44%) recorded the lowest WAASBY scores, while G2 (44.01%) displayed intermediate behavior with moderate adaptability and performance. These results support the use of WAASBY as a robust selection tool in multi-environment trials (Figure 12).

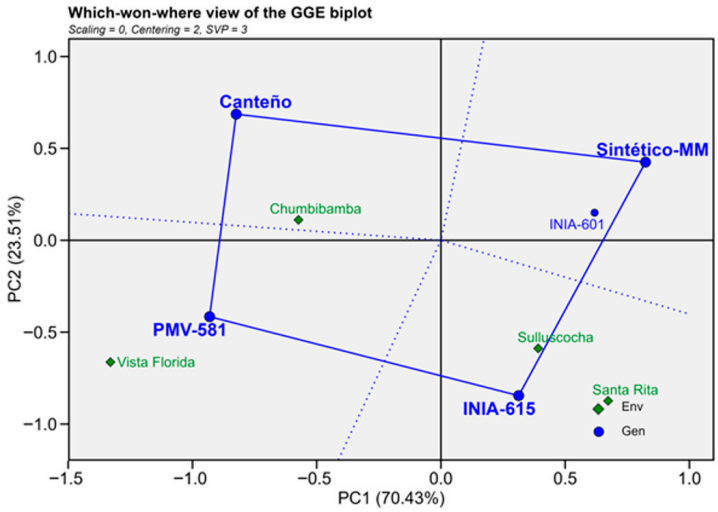

Figure 11. Which-won-where view of the GGE biplot for grain yield. The polygon connects the genotypes located farthest from the biplot origin, creating sectors.

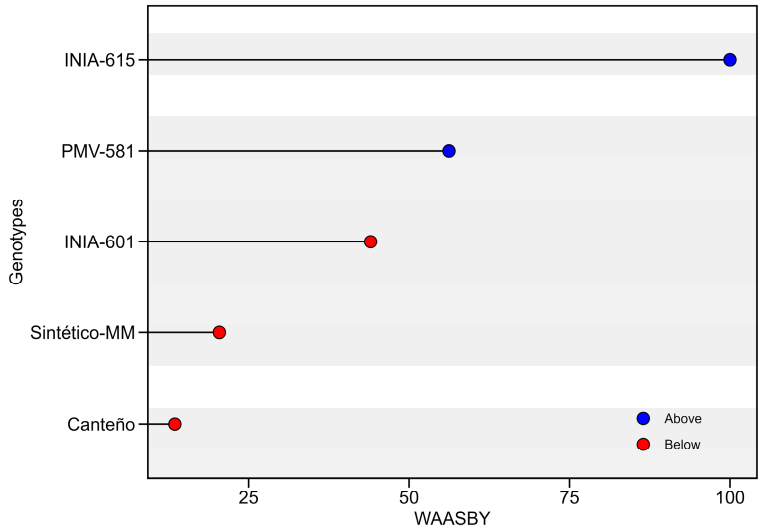

Figure 12. WAASBY index for genotype ranking based on grain yield and stability. The horizontal axis reports the WAASBY value, an integrated measure in which higher scores denote a more desirable combination of grain-yield performance and stability, while the vertical axis lists genotypes in descending order of WAASBY. WAASBY values, expressed on a 0–100% scale. Points are color-coded relative to the overall WAASBY mean (blue = above-average; red = below-average).

Finally, the Y × WAAS biplot allowed for the simultaneous evaluation of genotypic performance and stability across environments. Genotype G3 was positioned in quadrant IV, indicating high grain yield combined with strong stability, making it the most desirable selection. In contrast, G4, located in quadrant II, demonstrated high performance but lower stability. G5 displayed intermediate behavior with moderate yield and stability, whereas G1 exhibited a grain yield slightly above the overall mean but with low stability. Among environments, Vista Florida and Santa Rita were the most productive but also contributed to greater variability, while Sulluscocha was less favorable due to its low discriminative capacity and reduced performance. Notably, Chumbibamba, located in quadrant IV, exhibited both favorable average performance and low interaction with genotypes, indicating its suitability as a stable testing location for genotype evaluation. (Figure 13).

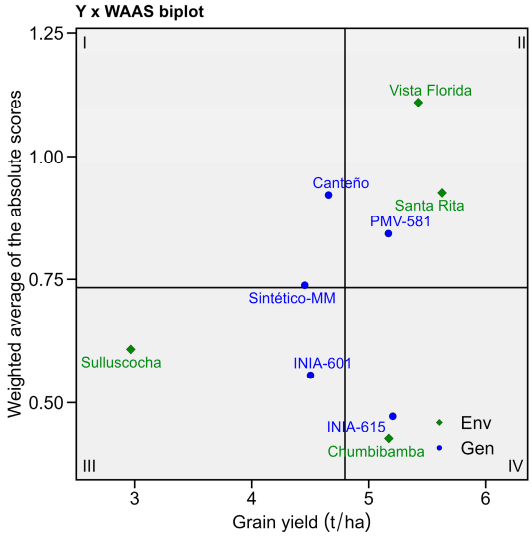

Figure 13. Y × WAAS biplot for field weight (kg), classifying genotypes and environments into four quadrants based on performance. The horizontal axis represents the mean field weight, while the vertical axis reflects the weighted average of the absolute scores (WAAS), where lower values indicate greater stability.

4. Discussion

This study demonstrated a significant genotype × environment (G × E) interaction for grain yield in purple corn, consistent with extensive evidence in maize that environment is often the dominant source of variation in multi-location trials [39]. In our trials across four contrasting Peruvian agro-ecological zones, the environmental effect on yield was pronounced, whereas genotypic differences, though significant, were comparatively smaller—a trend also observed by Ma et al. [40], who reported that environment accounted for ~50% of yield variation while genotype explained only ~4%. Such a large environmental influence underscores the importance of multi-environment testing to reliably identify broadly adapted, high-yielding genotypes. Similar conclusions were drawn by Mohammadi et al. [41], who reported that the largest proportion of total variation in multi-environment trials is attributed to environments, whereas G and G × E sources of variation are relatively smaller. G × E often causes rank changes in genotypes across sites, complicating direct selection. Therefore, stability analysis tools like AMMI and GGE biplots were employed, as they are widely used to dissect G × E patterns in maize. These biplot methods complement each other and have proven effective for evaluating yield stability and adaptation in maize and other crops. In fact, combining AMMI and GGE analyses can provide a more robust identification of optimal genotypes and target environments, which motivated the present multi-pronged approach (including WAASBY and Y × WAAS indices) to ensure comprehensive stability assessment.

Recent multi-environment evaluations conducted by Medina-Hoyos et al. [2] in the department of Cajamarca, involving the genotypes INIA-615, PMV-581, Canteño, and Sintético-MM, reported patterns consistent with those observed in the present study. In that research, INIA-615 exhibited high yield and phenotypic stability, surpassing PMV-581, Sintético-MM, and Canteño, while the latter two genotypes showed lower performance and adaptability. These results are in close agreement with our findings, confirming the reproducibility of genotype responses under different environmental contexts.

The present study extends this previous work by evaluating the same genetic materials across four contrasting Peruvian agro-ecological zones. This broader environmental coverage, combined with the implementation of advanced multivariate stability models

(AMMI, GGE, WAASBY, and Y × WAAS), provides a more comprehensive understanding of the genotype × environment (G × E) interaction and phenotypic stability in purple corn.

Although environments were clearly the dominant source of variation, it is important to recognize that several uncontrolled micro-environmental factors could also have influenced yield stability. Differences in temperature regimes, rainfall distribution, soil moisture, and local microclimates among test sites likely contributed to the observed environmental variance. For instance, even small variations in precipitation timing or soil water retention can affect pollination efficiency and kernel development in maize. Likewise, temperature fluctuations (e.g., during flowering) may alter metabolic and physiological responses, thereby modifying grain yield [42–44].

Previous reports on purple corn demonstrated that minimum temperature and relative humidity were strongly correlated with both cob weight and total anthocyanin content [45], with the highest anthocyanin concentrations occurring under cooler conditions. Such evidence supports the notion that climatic variability, particularly thermal and hydric fluctuations, can markedly influence phenotypic performance and biochemical composition in purple corn.

Although anthocyanin concentration was not quantified in the present study, its physiological relevance remains essential for interpreting the performance of purple corn genotypes across contrasting environments. Anthocyanins function beyond their nutritional and commercial value; they act as stress-responsive metabolites that protect plant tissues under high radiation, low temperatures, and oxidative conditions. Extensive evidence indicates that anthocyanin biosynthesis is activated through ROS-mediated signaling cascades during drought, salinity, excess light, cold, and heavy metal exposure, contributing to tolerance via enhanced antioxidant capacity, photoprotection, and osmotic adjustment [46–49].

In purple corn, recent studies provide clear mechanistic links between anthocyanin accumulation, environmental cues, and agronomic performance. Soto Aquino et al. [45] demonstrated that minimum temperature and relative humidity strongly influence anthocyanin concentration and cob morphological traits, with colder environments promoting both higher pigment accumulation and favorable cob characteristics. Likewise, Medina-Hoyos et al. [2] reported that anthocyanin-rich genotypes, such as INIA 601, achieve higher grain production across diverse environments, suggesting that pigment biosynthesis may support physiological resilience under fluctuating field conditions. These findings align with broader evidence that genotypes with elevated anthocyanin levels often maintain more stable reproductive performance when exposed to environmental variation.

Thus, environments that induce anthocyanin biosynthesis, such as the highland sites evaluated in this study, may concurrently favor yield stability in elite genotypes like INIA 615. Incorporating anthocyanin profiling into future multi-environment trials will help determine whether stress-mitigation mechanisms associated with pigment metabolism contribute directly to the broad adaptation observed in the most stable purple corn genotypes.

In the present study, while the genotype × environment interaction for plant height was not statistically significant, exploratory GGE biplot analysis revealed latent patterns of adaptation. Genotypes such as INIA-615 and PMV-581 occupied polygon vertices, suggesting differential behavior in specific environments such as Santa Rita. This observation parallels the findings of [50,51], who emphasized that even in the absence of statistically significant interaction terms, GGE biplots remain a valuable tool for visualizing adaptation trends and guiding genotype deployment under diverse agro-ecological conditions.

Despite the strong G × E, certain genotypes in this study displayed superior performance and stability. Notably, INIA-615 emerged as the most productive and stable genotype across all environments, followed by G4 (PMV-581). These improved genotypes maintained high mean yields with minimal fluctuation, indicating broad adaptation. Such

wide adaptability is a key breeding goal in maize, identifying genotypes that consistently outperform others across diverse conditions [41,52,53]. Our findings align with those of other authors who found that a few elite hybrids could combine high yield with stability in multi-environment trials [27,54–56]. For example, ZF-2208 and DY-519 were top-performing and stable hybrids across ten environments in China, reinforcing the notion that certain genotypes possess broad adaptability [54]. In contrast, some other entries (e.g., the local landrace Canteño or the synthetic Sintético-MM) showed more variable performance, suggesting specific adaptation to particular environments. This pattern is commonly observed: landrace or unadapted genotypes may excel in their home environments but perform inconsistently elsewhere, whereas improved lines like INIA-615 exhibit dynamic stability (the ability to maintain above-average yield across environments) [57]. Broadly adapted genotypes likely possess stress-tolerance traits and plasticity that buffer against environmental variation, an effect noted by Duvick [58] and others in modern maize hybrids selected for stress resilience [59]. Indeed, decades of breeding have increased maize's general stress tolerance, contributing to yield gains under both optimal and stressful conditions [60,61].

The GGE "which-won-where" biplot further elucidated genotype–environment specificity: INIA-615 excelled in Santa Rita and Sulluscocha, PMV-581 in Vista Florida and Chumbibamba, whereas Sintético-MM and INIA-601 clustered near the origin, confirming broad adaptability. Ma et al. [40]. identified DY-519 and JG-18 as winners in specific environments in 2022, and ZF-2208 and ZF-2210 in 2023. Likewise, Katsenios et al. [25] delineated three mega-environments in Greece and matched GEN2, GEN4, and GEN5 to them, demonstrating how multi-environment AMMI biplots guide site-specific cultivar recommendation.

The use of the WAASBY index and the Y × WAAS biplot in our analysis provided additional insight into genotype stability. The WAASBY index [30] integrates yield performance and stability into a single metric by assigning weights to each. This approach builds on earlier selection indices (e.g., Kang's yield-stability rank sum; Kang, [62]) to facilitate simultaneous selection for high yield and low G × E variance. In our results, the WAASBY index clearly favored INIA-615, confirming that it had the best balance of productivity and stability, followed by PMV-581 and INIA-601. The Y × WAAS biplot visualized this trade-off effectively. As described by Olivoto et al. [30], such biplots separate genotypes into four quadrants: (I) unstable and low-yielding, (II) unstable but high-yielding, (III) stable but low-yielding, and (IV) stable and high-yielding (ideal). In our case, INIA-615 and PMV-581 fell in the desirable quadrant IV (broadly adapted, "winner" genotypes), whereas other entries either had lower yields or specific adaptability. The concurrence among AMMI, GGE, and WAASBY results in identifying INIA-615 as superior lends confidence to its recommendation for wide cultivation. Furthermore, the agreement of multiple stability metrics in our study mirrors findings in other maize research. For instance, a stability analysis of tropical maize hybrids by Mafouasson et al. (2018) [39] also found that AMMI and GGE biplots identified broadly adapted, high-yield genotypes, while stability indices aided in rank confirmation. Overall, our G × E analysis indicates that the improved purple corn cultivar INIA-615 possesses an outstanding combination of high yield and phenotypic stability across environments—a critical attribute for food security in variable climates.

It is worth noting that our study focused on purple corn, a crop of growing interest due to its anthocyanin content, yet the G × E interaction patterns observed are comparable to those in conventional (yellow/white) maize. Recent work in Peru's highland and coastal zones has similarly highlighted the importance of multi-environment testing for purple corn. For example, Medina-Hoyos et al. [2] evaluated diverse purple corn cultivars across Andean locations and identified certain improved varieties with both high grain yield and elevated anthocyanin content that were specifically adapted to the Cajamarca highlands.

Such findings underscore that even for specialty maize, such as purple corn, breeding for broad adaptation and stability is achievable. In our study, the superior performance of INIA-615 (an improved INIA release) across various environments suggests that modern breeding has significantly enhanced the adaptability of purple corn, extending its range beyond its traditional niche. Nevertheless, genotype ranking can still change with location due to interactions with altitude, climate, and soils. Multi-site trials in other studies have indeed found crossover interactions for certain genotypes—i.e., a different variety becomes top-yielding in a particular environment [63–65]. In our results, no extreme crossover was evident for the top genotypes (their superiority was consistent), which is an ideal scenario for selecting generally adapted cultivars. This is corroborated by Pour-Aboughadareh et al. [66], who noted that when a genotype consistently ranks high across sites, it can be confidently promoted for wide cultivation despite diverse growing conditions. Overall, our findings, in line with the literature, highlight that the development of high-yielding, phenotypically stable purple corn varieties like INIA-615 can greatly facilitate their recommendation for cultivation in diverse regions, ensuring farmers a more predictable performance year to year.

Apart from yield, our study evaluated key physiological traits linked to stress adaptation, notably the anthesis–silking interval (ASI). ASI, the time gap between pollen shed (anthesis) and silk emergence is a sensitive indicator of flowering synchrony, and it is well known to widen under stress conditions such as drought or heat. In maize, water or nutrient stress often delays silk emergence more than pollen shed, causing ASI to increase and leading to poor pollination and kernel set [67,68]. Bolaños and Edmeades [69] demonstrated that an extended ASI under drought is a primary cause of yield failure in tropical maize, as it reflects the plant's inability to timely support silking due to stress. In our multi-environment trials, differences in ASI among genotypes were observed and tended to correlate inversely with performance stability: the most stable, high-yield genotypes (INIA-615 and PMV-581) maintained relatively short ASI values even in harsher environments, whereas less stable lines showed larger ASI shifts (indicative of stress susceptibility). This result agrees with the paradigm that shorter ASI under stress denotes better tolerance. Genotypes that can keep ASI short are more likely to ensure pollination and grain fill under adverse conditions, thus buffering yield [67,70]. Breeding programs routinely use ASI as a secondary trait for selecting drought-tolerant maize [71]. Indeed, selection for reduced ASI has been instrumental in developing tropical maize populations with improved drought resilience [72]. Bänziger et al. [11] and other researchers at CIMMYT have reported that modern drought-bred maize varieties show dramatically shorter ASI and higher kernel set under stress compared to older germplasm. The present findings concur: the top-performing genotypes had the smallest ASI, implying they possess superior stress-tolerance mechanisms likely inherited from their breeding pedigree.

It is notable that INIA-615, the most stable genotype, likely benefitted from such traits. As an improved line, INIA-615 was probably selected under both optimal and stress conditions, resulting in a phenotype that minimizes flowering delay when resources are limiting. This is supported by the general observation that newer maize hybrids sustain reproductive growth better under stress than older ones. For example, Araus et al. [59] documented that modern hybrids flower with little delay and maintain sink development during drought, whereas older varieties suffer silk delay and barrenness. In this study, INIA-615's consistently short ASI across environments suggests an intrinsic tolerance (e.g., efficient partitioning of assimilates to the ear around flowering) that contributes to its yield stability. Meanwhile, a genotype with a long ASI (e.g., if any entry showed pronounced silk delay in a particular site) would likely experience reduced kernel number and yield in that environment, reflecting a G × E interaction driven by stress sensitivity. We indeed

observed that environments with harsher conditions (e.g., possibly a drier season or poorer soil in one test site) induced longer ASI and yield drops in the more sensitive genotypes, but not in INIA-615. This resilience is characteristic of drought-tolerant maize and aligns with previous studies: shorter ASI has been genetically associated with higher grain yield under stress and is often genetically correlated with other adaptive traits like increased silk growth rate and reduced tassel size [73,74]. Moreover, Edmeades [75] noted that over 50 years of maize breeding, one consistent physiological change in modern hybrids is a reduction in ASI under stress, which has contributed significantly to yield stability in variable climates. The present results add further evidence that ASI is a useful phenotypic marker of stability; the genotypes that excelled across Peruvian environments did so, at least in part, by avoiding large ASI values (and the associated pollination failures) in unfavorable conditions.

Ear-rot incidence, caused primarily by fungal pathogens (e.g., *Fusarium* spp.), was another critical factor evaluated in this study. Ear rots are a major concern for maize production in Peru and globally, as they not only reduce yield and grain quality but also can contaminate grain with mycotoxins [76]. In our multi-location trials, we observed genotype differences in ear-rot resistance, as well as environmental influences on disease severity. Notably, INIA-615 again stood out by showing one of the lowest incidences of ear rot across environments, suggesting that this genotype carries some level of genetic resistance in addition to its high yield. In contrast, certain other genotypes (for instance, if Canteño or Sintético-MM exhibited higher ear-rot levels in humid environments) were more susceptible, especially under conditions conducive to disease (e.g., high moisture and warm temperatures at lower-altitude sites). This genotype ranking for ear-rot resistance appears to be relatively consistent across the test environments—a resistant genotype tended to remain among the least affected in each location, and a susceptible one remained prone—indicating a lack of major crossover interaction for disease reaction. Such stability in resistance is a positive finding, as it implies that breeding for ear-rot resistance can yield benefits across diverse environments. Indeed, other studies have shown that some maize hybrids express "stable" resistance to ear rots, meaning their relative performance (in terms of disease severity) does not drastically change with environment [77]. For example, a recent multi-environment evaluation by Lana et al. [78] found that most tested hybrids had a consistent ranking for *Gibberella* ear-rot resistance across sites (little crossover G × E), even though absolute disease levels varied. The results of the present research are in line with this: genotypes like INIA-615 maintained low disease in all zones, whereas more susceptible entries were consistently hit by ear rot whenever conditions favored the pathogen.

Although the multi-environment dataset generated in this study provides valuable insights, several limitations must be acknowledged to contextualize the findings. The experiment was conducted during a single growing season and included a restricted number of purple corn genotypes, which limits the extent to which the results can be generalized across years and the broader diversity of Andean germplasm. Furthermore, physiological and biochemical traits closely associated with stress resilience, such as anthocyanin concentration, antioxidant capacity, and root architectural plasticity, were not measured. Given that anthocyanins can mitigate oxidative stress and contribute to reproductive stability under environmental fluctuations, the lack of these measurements constrains a mechanistic interpretation of the superior performance observed in certain genotypes. Future studies should incorporate multi-year trials, a broader genetic panel, and the quantification of anthocyanins and key physiological attributes to better elucidate the drivers of yield stability and adaptation in purple corn.

From a breeding and agronomy standpoint, the present results emphasize the value of integrated selection for yield, stability, and disease resistance. The genotype INIA-615

exemplifies this integration: it not only yielded the highest and was most stable, but also had the shortest ASI and lowest ear rot incidence—a combination of traits that is highly desirable for sustainable production. Such a genotype can be recommended as a candidate for variety release in multiple regions, given its broad adaptation and resilience to stresses both abiotic (drought/heat, as inferred from ASI) and biotic (ear-rot disease). Future research could further validate its performance over more years and include assessments of other diseases (e.g., foliar blights, stalk rots) and nutritional quality (anthocyanin levels), to fully characterize its potential as a commercial purple corn variety. Moreover, this study highlights the utility of advanced analytic tools (GGE biplots, WAASBY indices) in multi-trait, multi-environment datasets, and breeders can identify "all-round" superior genotypes efficiently. As climate variability increases disease and drought pressures, the approach used here, which evaluates genotype stability across environments and under multiple stress factors, will be crucial for developing next-generation maize cultivars. In summary, the convergence of evidence from the present trials and prior studies leads to a clear conclusion: INIA-615 (followed by PMV-581) is a robust purple corn genotype combining high yield potential, phenotypic stability, stress-tolerance traits like short ASI, and resistance to ear rot. Such genotypes will be instrumental in improving and expanding the cultivation of purple corn in diverse agro-ecological zones of Peru and beyond, ensuring both high productivity and reliability for farmers.

5. Conclusions

This study demonstrated that environmental variation was the dominant factor shaping phenotypic performance in purple corn, yet significant genotype × environment interactions justified the use of AMMI, GGE, WAASBY, and Y × WAAS models to identify genotypes with superior adaptability and stability.

Among the five evaluated genotypes, INIA-615 exhibited the most favorable combination of high yield, low ear-rot incidence, and a short anthesis–silking interval. These attributes collectively indicate its broad adaptability, resilience to environmental stress, and suitability for wide cultivation. Given the cold, high-altitude conditions of Sullus-cocha (minimum: 3 °C) and the cool, humid environment of Chumbibamba (10.3–13.3 °C), INIA-615 represents a practical option for farmers in these areas because of its stable performance under low temperatures and its reduced susceptibility to ear rot. In contrast, PMV-581 demonstrated strong site-specific performance, particularly under favorable conditions, indicating its potential for targeted recommendation in high-yield environments. Meanwhile, INIA-601 and Sintético-MM displayed moderate productivity but greater phenotypic stability, which may be advantageous in marginal or variable production systems, whereas Canteño remained locally adapted but less stable, reinforcing its role as a regional genotype rather than a broadly adapted cultivar.

The convergence of multiple stability indices confirms INIA-615 as a robust candidate for multi-environment cultivation in Peru, with potential to enhance farmer productivity and contribute to the expansion of the purple corn value chain. Future research should explore genomic-assisted selection and molecular characterization of INIA-615 to identify loci associated with stability and productivity. Combining phenotypic data with genomic information will strengthen decision-making in advanced breeding cycles and contribute to the development of superior purple corn cultivars adapted to climate change.

Supplementary Materials: The following supporting information can be downloaded at: https://www.mdpi.com/article/10.3390/ijpb17010003/s1, Figure S1. Schematic layout of the field experiment organized as a randomized complete block design with three replicates (Blocks I–III). Each plot (5 m long) was sown with one of five treatments: G1 = Canteño, G2 = INIA 601, G3 = INIA 615, G4 = PMV 581 and G5 = Synthetic MM. Plots within blocks were spaced 3.2 m apart, with 1 m alleys

separating blocks and 0.80 m border strips surrounding the entire experimental area, experimental unit (16 m^2); Figure S2. AMMI stability value (ASV) plotted against plant height (cm) for each genotype; Figure S3. AMMI stability value (ASV) plotted against anthesis–silking interval (ASI, in days) for each genotype; Figure S4. AMMI stability value (ASV) plotted against Cob rot incidence (%) for each genotype; Figure S5. AMMI stability value (ASV) plotted against Field weight (kg) for each genotype; Figure S6. AMMI stability value (ASV) plotted against Grain yield (t/ha) for each genotype; Table S1. The AMMI analysis of variance for Plant height (cm) over four environments; Table S2. The AMMI analysis of variance Anthesis–Silking Interval (ASI) over four environments; Table S3. The AMMI analysis of variance Cob rot % over four environments; Table S4. The AMMI analysis of variance for Field Weight (kg) over four environments; Table S5. The AMMI analysis of variance for grain yield (t/ha) over four environments.

Author Contributions: Conceptualization, G.G., M.E.T., W.V. and Y.R.; methodology, G.G., M.E.T., W.V. and Y.R.; validation, G.G., M.E.T., W.V. and Y.R.; formal analysis, D.M.; investigation, G.G., M.E.T., W.V. and Y.R.; resources, F.M., F.E., A.V. and S.A.; data curation, G.G., M.E.T., W.V. and Y.R.; writing—original draft preparation, D.M. and H.C.-S.; writing—review and editing, D.M. and H.C.-S.; visualization, D.M.; supervision, D.M.; project administration, O.P., F.M., F.E., A.V. and S.A.; funding acquisition, O.P. All authors have read and agreed to the published version of the manuscript.

Funding: "Adaptability, Yield Stability, and Agronomic Performance of Improved Purple Corn (*Zea mays* L.) Hybrids across Diverse Agro-ecological Zones in Peru" was funded by the investment Project 2361771: "Improving the availability, access, and use of quality seeds for potato, amylaceous maize, grain legumes, and cereals in the regions of Junín, Ayacucho, Cusco, and Puno (4 departments)", supported by Instituto Nacional de Innovación Agraria (INIA) Peru.

Informed Consent Statement: Not applicable.

Data Availability Statement: The data presented in this study are available on request from the corresponding authors.

Conflicts of Interest: The authors declare no conflicts of interest.

References

1. Ministerio del Ambiente (MINAM). *Línea de Base de la Diversidad Genética del Maíz Peruano con Fines de Bioseguridad*; Grupo Raso: Lima, Perú, 2018; 144p.
2. Medina, A.; Narro, L.; Chávez, A. Cultivo de maíz morado (*Zea mays* L.) en zona altoandina de Perú: Adaptación e identificación de cultivares de alto rendimiento y contenido de antocianina. *Sci. Agropecu.* **2020**, *11*, 291–299. [CrossRef]
3. Pedreschi, R.; Cisneros-Zevallos, L. Antioxidant phytochemicals and oxidative stress: A review. *Food Sci. Technol. Int.* **2007**, *13*, 277–288. [CrossRef]
4. Xu, D.; Hu, M.J.; Wang, Y.Q.; Cui, Y.L. Antioxidant activities of quercetin and its complexes for medicinal application. *Molecules* **2019**, *24*, 1123. [CrossRef] [PubMed]
5. Coșarcă, S.; Tanase, C.; Muntean, D.L. Therapeutic aspects of catechin and its derivatives—An update. *Acta Biol. Marisiensis* **2019**, *2*, 21–29. [CrossRef]
6. Felter, S.P.; Zhang, X.; Thompson, C. Butylated hydroxyanisole: Carcinogenic food additive to be avoided or harmless antioxidant important to protect food supply? *Regul. Toxicol. Pharmacol.* **2021**, *121*, 104887. [CrossRef]
7. Shi, N.; Chen, X.; Chen, T. Anthocyanins in colorectal cancer prevention review. *Antioxidants* **2021**, *10*, 1600. [CrossRef]
8. Dong, Y.; Wu, X.; Han, L.; Bian, J.; He, C.; El-Omar, E.; Wang, M. The potential roles of dietary anthocyanins in inhibiting vascular endothelial cell senescence and preventing cardiovascular diseases. *Nutrients* **2022**, *14*, 2836. [CrossRef]
9. MIDAGRI. *Análisis de Mercado: 2015–2021. Maíz Morado*; MIDAGRI: Lima, Perú, 2022. Available online: https://www.gob.pe/institucion/agromercado/informes-publicaciones/2624383-analisis-de-mercado-maiz-morado-2015-2021 (accessed on 12 November 2025).
10. Yue, H.; Olivoto, T.; Bu, J.; Wei, J.; Liu, P.; Wu, W.; Nardino, M.; Jiang, X. Assessing the role of genotype by environment interaction as determinants of maize grain yield and lodging resistance. *BMC Plant Biol.* **2025**, *25*, 120. [CrossRef]
11. Bänziger, M.; Cooper, M. Breeding for low-input conditions and consequences for participatory plant breeding: Examples from tropical maize and wheat. *Euphytica* **2001**, *122*, 503–519. [CrossRef]
12. Yan, W.; Holland, J.B. A heritability-adjusted GGE biplot for test environment evaluation. *Euphytica* **2010**, *171*, 355–369. [CrossRef]

13. Cooper, M.; Messina, C.D.; Podlich, D.; Totir, L.R.; Baumgarten, A.; Hausmann, N.J.; Graham, G. Predicting the future of plant breeding: Complementing empirical evaluation with genetic prediction. *Crop Pasture Sci.* **2014**, *65*, 311–336. [CrossRef]
14. Fu, Y.B.; Cheng, B.; Peterson, G.W. Genetic diversity analysis of yellow mustard (*Sinapis alba* L.) germplasm based on genotyping by sequencing. *Genet. Resour. Crop Evol.* **2014**, *61*, 579–594. [CrossRef]
15. Yadesa, L. Review on genetic-environmental interaction (GxE) and its application in crop breeding. *Int. J. Res. Agron.* **2022**, *5*, 95–101. [CrossRef]
16. Ndiaye, M.; Adam, M.; Ganyo, K.K.; Guissé, A.; Cissé, N.; Muller, B. Genotype–Environment Interaction: Trade-Offs between the Agronomic Performance and Stability of Dual-Purpose Sorghum (*Sorghum bicolor* L. Moench) Genotypes in Senegal. *Agronomy* **2019**, *9*, 867. [CrossRef]
17. Lee, S.Y.; Lee, H.-S.; Lee, C.-M.; Ha, S.-K.; Park, H.-M.; Lee, S.-M.; Kwon, Y.; Jeung, J.-U.; Mo, Y. Multi-Environment Trials and Stability Analysis for Yield-Related Traits of Commercial Rice Cultivars. *Agriculture* **2023**, *13*, 256. [CrossRef]
18. Duvick, D.N. The Contribution of Breeding to Yield Advances in maize (*Zea mays* L.). *Adv. Agron.* **2005**, *86*, 83–145. [CrossRef]
19. Epinat-Le Signor, C.; Dousse, S.; Lorgeou, J.; Denis, J.; Bonhomme, R.; Carolo, P.; Charcosset, A. Interpretation of genotype x environment interactions for early maize hybrids over 12 years. *Crop Sci.* **2001**, *41*, 663–669. [CrossRef]
20. Lu'quez, J.E.; Aguirrezábal, L.A.N.; Agüero, M.E.; Pereyra, V.R. Stability and adaptability of cultivars in non-balanced yield trials: Comparison of methods for selecting 'high oleic' sunflower hybrids for grain yield and quality. *J. Agron. Crop Sci.* **2002**, *188*, 225–234. [CrossRef]
21. Yan, W.; Kang, M.S.; Ma, B.; Woods, S.; Cornelius, P.L. GGE Biplot vs. AMMI Analysis of Genotype-by-Environment Data. *Crop Sci.* **2007**, *47*, 643–653. [CrossRef]
22. Gauch, H.G. A simple protocol for AMMI analysis of yield trials. *Crop Sci.* **2013**, *53*, 1860–1869. [CrossRef]
23. Yohane, E.N.; Shimelis, H.; Laing, M.; Mathew, I.; Shayanowako, A. Genotype-by-environment interaction and stability analyses of grain yield in pigeonpea [*Cajanus cajan* (L.) Millspaugh]. *Acta Agric. Scand. Sect. B Soil Plant Sci.* **2021**, *71*, 145–155. [CrossRef]
24. Singamsetti, A.; Shahi, J.P.; Zaidi, P.H.; Seetharam, K.; Vinayan, M.T.; Kumar, M.; Madankar, K. Genotype × environment interaction and selection of maize (*Zea mays* L.) hybrids across moisture regimes. *Field Crops Res.* **2021**, *270*, 108224. [CrossRef]
25. Katsenios, N.; Sparangis, P.; Leonidakis, D.; Katsaros, G.; Kakabouki, I.; Vlachakis, D.; Efthimiadou, A. Effect of Genotype × Environment Interaction on Yield of Maize Hybrids in Greece Using AMMI Analysis. *Agronomy* **2021**, *11*, 479. [CrossRef]
26. Shojaei, S.H.; Mostafavi, K.; Omrani, A.; Omrani, S.; Nasir Mousavi, S.M.; Illés, Á.; Nagy, J. Yield stability analysis of maize (*Zea mays* L.) hybrids using parametric and AMMI methods. *Scientifica* **2021**, *2021*, 5576691. [CrossRef]
27. Bocianowski, J.; Nowosad, K.; Rejek, D. Genotype–environment interaction for grain yield in maize (*Zea mays* L.) using the additive main effects and multiplicative interaction (AMMI) model. *J. Appl. Genet.* **2024**, *65*, 653–664. [CrossRef]
28. Rodríguez-Pérez, G.; García-Ramírez, A.; Reynaga-Franco, F.J.; Mendívil-Mendoza, J.E.; Ochoa Meza, A.R.; Cervantes-Ortiz, F.; Andrio Enriquez, E. Rendimiento y componentes agronómicos en híbridos de maíz morado (*Zea mays* L.) usando el modelo AMMI. *An. Cienc.* **2023**, *84*, 54–67. [CrossRef]
29. Zobel, R.W.; Wright, M.J.; Gauch, H.G. Statistical analysis of a yield trial. *Agron. J.* **1988**, *80*, 388–393. [CrossRef]
30. Olivoto, T.; Lúcio, A.D.C.; Da Silva, J.A.G.; Sari, B.G.S.; Diel, M.I. Mean performance and stability in multi-environment trials II: Selection based on multiple traits. *Agron. J.* **2019**, *111*, 2961–2969. [CrossRef]
31. Yan, W.; Tinker, N.A. Biplot analysis of multi-environment trial data: Principles and applications. *Can. J. Plant Sci.* **2006**, *86*, 623–645. [CrossRef]
32. Olivoto, T.; Lúcio, A.D. metan: An R package for multi-environment trial analysis. *Methods Ecol. Evol.* **2020**, *11*, 783–789. [CrossRef]
33. Abate, M. Genotype by environment interaction and yield stability analysis of open pollinated maize varieties using AMMI model in Afar Regional State, Ethiopia. *J. Plant Breed. Crop Sci.* **2020**, *12*, 8–15. [CrossRef]
34. Abanto, W.; Medina, A.; Injante, P. *Maíz Morado INIA 601: Variedad de Maíz Morado para la Sierra Norte del Perú*; Plegable No. 3-2014; Instituto Nacional de Innovación Agraria (INIA): Cajamarca, Perú, 2014. Available online: https://repositorio.inia.gob.pe/handle/20.500.12955/65 (accessed on 12 November 2025).
35. Estación Experimental Agraria Cañaán–Ayacucho. *Maíz INIA 615—Negro Cañaán: Nueva Variedad de Maíz Morado para la Sierra Peruana*; Instituto Nacional de Innovación Agraria (INIA): Lima, Perú, 2007. Available online: https://repositorio.inia.gob.pe/handle/20.500.12955/648 (accessed on 12 November 2025).
36. Atalaya, M.R.; Hoyos, A.M. Estudio comparativo de las características agronómicas y químicas de tres cultivares de maíz morado en Perú. *Rev. Mex. Cienc. Agric.* **2022**, *13*, 953–964. [CrossRef]
37. Quevedo, W.S. *Maíz Blanco Urubamba (Blanco Gigante Cuzco)*; Manual Técnico No. 13; Instituto Nacional de Innovación Agraria (INIA): Cusco, Perú, 2013. Available online: https://repositorio.inia.gob.pe/handle/20.500.12955/87 (accessed on 11 November 2025).
38. Manrique, A. *El Maíz Morado Peruano*; Instituto Nacional de Innovación Agraria (INIA): Lima, Perú, 2000. Available online: https://repositorio.inia.gob.pe/items/d5d896b6-4487-4f07-99fa-29cf2b02fcad (accessed on 12 November 2025).

39. Mafouasson, H.N.A.; Gracen, V.; Yeboah, M.A.; Ntsomboh-Ntsefong, G.; Tandzi, L.N.; Mutengwa, C.S. Genotype-by-Environment Interaction and Yield Stability of Maize Single Cross Hybrids Developed from Tropical Inbred Lines. *Agronomy* **2018**, *8*, 62. [CrossRef]
40. Ma, C.; Liu, C.; Ye, Z. Influence of genotype × environment interaction on yield stability of maize hybrids with AMMI model and GGE biplot. *Agronomy* **2024**, *14*, 1000. [CrossRef]
41. Mohammadi, R.; Amri, A.; Haghparast, R.; Sadeghzadeh, D.; Armion, M.; Ahmadi, M.M. Pattern analysis of genotype-by-environment interaction for grain yield in durum wheat. *J. Agric. Sci.* **2009**, *147*, 537–545. [CrossRef]
42. Waqas, M.A.; Wang, X.; Zafar, S.A.; Noor, M.A.; Hussain, H.A.; Nawaz, M.A.; Farooq, M. Thermal stresses in maize: Effects and management strategies. *Plants* **2021**, *10*, 293. [CrossRef]
43. Maitah, M.; Malec, K.; Maitah, K. Influence of precipitation and temperature on maize production in the Czech Republic from 2002 to 2019. *Sci. Rep.* **2021**, *11*, 10467. [CrossRef]
44. López Hernández, N.A.; Martínez Sifuentes, A.R.; Halecki, W.; Trucíos Caciano, R.; Rodríguez Moreno, V.M. An assessment of the impact of climate change on maize production in northern Mexico. *Atmosphere* **2025**, *16*, 455. [CrossRef]
45. Soto-Aquino, V.; Ignacio-Cárdenas, S.; Japa-Espinoza, A.J.; Campos-Félix, U.; Ciriaco-Poma, J.; Campos-Félix, A.; Pantoja-Medina, B.; Dávalos-Prado, J.Z. Influence of climatic parameters and plant morphological characters on the total anthocyanin content of purple maize (*Zea mays* L., PMV-581) cob core. *Agronomy* **2024**, *14*, 2021. [CrossRef]
46. Nakabayashi, R.; Saito, K. Integrated metabolomics for abiotic stress responses in plants. *Curr. Opin. Plant Biol.* **2015**, *24*, 10–16. [CrossRef] [PubMed]
47. Naing, A.H.; Kim, C.K. Abiotic stress-induced anthocyanins in plants: Their role in tolerance to abiotic stresses. *Physiol. Plant.* **2021**, *172*, 1711–1723. [CrossRef]
48. Kovinich, N.; Kayanja, G.; Chanoca, A.; Otegui, M.S.; Grotewold, E. Abiotic stresses induce different localizations of anthocyanins in *Arabidopsis*. *Plant Signal. Behav.* **2015**, *10*, e1027850. [CrossRef]
49. Yan, W.; Li, J.; Lin, X.; Wang, L.; Yang, X.; Xia, X.; Zhang, Y.; Yang, S.; Li, H.; Deng, X.; et al. Changes in plant anthocyanin levels in response to abiotic stresses: A meta-analysis. *Plant Biotechnol. Rep.* **2022**, *16*, 497–508. [CrossRef]
50. Mitrović, B.; Stanisavljević, D.; Treski, S.; Stojaković, M.; Ivanović, M.; Bekavac, G.; Rajković, M. Evaluation of experimental maize hybrids tested in multi-location trials using AMMI and GGE biplot analyses. *Turk. J. Field Crop* **2012**, *17*, 35–40.
51. Hongyu, K.; García-Peña, M.; Araújo, L.; Santos Dias, C. Statistical analysis of yield trials by AMMI analysis of genotype–environment interaction. *Biom. Lett.* **2014**, *51*, 89–102. [CrossRef]
52. Bernardo Júnior, L.A.Y.; de Silva, C.P.; de Oliveira, L.A.; Nuvunga, J.J.; Pires, L.P.M.; Von Pinho, R.G.; Balestre, M. AMMI Bayesian Models to Study Stability and Adaptability in Maize. *Agron. J.* **2018**, *110*, 1765–1776. [CrossRef]
53. Braun, H.J.; Atlin, G.; Payne, T. Multi-location testing as a tool to identify plant response to global climate change. In *Climate Change and Crop Production*; Reynolds, M., Ed.; CABI: Wallingford, UK, 2010; pp. 115–138. [CrossRef]
54. Fan, X.; Kang, M.S.; Chen, H.; Zhang, Y.; Tan, J.; Xu, C. Yield Stability of Maize Hybrids Evaluated in Multi-Environment Trials in Yunnan, China. *Agron. J.* **2007**, *99*, 220–228. [CrossRef]
55. Santos, D.C.D.; Pereira, C.H.; Nunes, J.A.R.; Lepre, A.L. Adaptability and stability of maize hybrids in unreplicated multienvironment trials. *Rev. Ciênc. Agron.* **2019**, *50*, e20190010. [CrossRef]
56. Uberti, A.; Rezende, W.M.; Caixeta, D.G.; Reis, H.M.; Resende, N.C.V.; Destro, V.; DeLima, R.O. Assessment of yield performance and stability of hybrids and populations of tropical maize across multiple environments in Southeastern Brazil. *Crop Sci.* **2023**, *63*, 2012–2032. [CrossRef]
57. Dwivedi, S.L.; Ceccarelli, S.; Blair, M.W.; Upadhyaya, H.D.; Are, A.K.; Ortiz, R. Landrace Germplasm for Improving Yield and Abiotic Stress Adaptation. *Trends Plant Sci.* **2016**, *21*, 31–42. [CrossRef]
58. Duvick, D.N. What is yield? In *Developing Drought and Low N-Tolerant Maize, Proceedings of a Symposium, CIMMYT, El Batán, Mexico, 25–29 March 1996*; Edmeades, G.O., Bänziger, B., Mickelson, H.R., Peña-Valdivia, C., Eds.; CIMMYT: Mexico City, Mexico, 1997; pp. 332–335.
59. Araus, J.L.; Serret, M.D.; Edmeades, G.O. Phenotyping maize for adaptation to drought. *Front. Physiol.* **2012**, *3*, 305. [CrossRef]
60. Tollenaar, M.; Lee, E.A. Dissection of physiological processes underlying grain yield in maize by examining genetic improvement and heterosis. *Maydica* **2006**, *51*, 399.
61. Prasanna, B.M.; Cairns, J.E.; Zaidi, P.H.; Beyene, Y.; Makumbi, D.; Gowda, M.; Magorokosho, C.; Zaman-Allah, M.; Olsen, M.; Das, A.; et al. Beat the stress: Breeding for climate resilience in maize for the tropical rainfed environments. *Theor. Appl. Genet.* **2021**, *134*, 1729–1752. [CrossRef]
62. Kang, M.S. A Rank-Sum Method for Selecting High-Yielding, Stable Corn Genotypes. *Cereal Res. Commun.* **1988**, *16*, 113–115.
63. Nyombayire, A.; Derera, J.; Sibiya, J.; Ngaboyisonga, C. Genotype × Environment Interaction and Stability Analysis for Grain Yield of Diallel Cross Maize Hybrids Across Tropical Medium and Highland Ecologies. *J. Plant Sci.* **2018**, *6*, 101–106.
64. Crossa, J.; Gauch, H.G., Jr.; Zobel, R.W. Additive Main Effects and Multiplicative Interaction Analysis of Two International Maize Cultivar Trials. *Crop Sci.* **1990**, *30*, 493–500. [CrossRef]

65. Ljubičić, N.; Popović, V.; Kostić, M.; Pajić, M.; Buđen, M.; Gligorević, K.; Dražić, M.; Bižić, M.; Crnojević, V. Multivariate Interaction Analysis of *Zea mays* L. Genotypes Growth Productivity in Different Environmental Conditions. *Plants* **2023**, *12*, 2165. [CrossRef]
66. Pour-Aboughadareh, A.; Khalili, M.; Poczai, P.; Olivoto, T. Stability indices to deciphering the genotype-by-environment interaction (GEI) effect: An applicable review for use in plant breeding programs. *Plants* **2022**, *11*, 414. [CrossRef]
67. Lima, D.C.; de Leon, N.; Kaeppler, S.M. Utility of anthesis–silking interval information to predict grain yield under water and nitrogen limited conditions. *Crop Sci.* **2022**, *63*, 151–163. [CrossRef]
68. Li, W.; Hao, Z.; Pang, J.; Zhang, M.; Wang, N.; Li, X.; Li, W.; Wang, L.; Xu, M. Effect of water-deficit on tassel development in maize. *Gene* **2019**, *681*, 86–92. [CrossRef] [PubMed]
69. Bolaños, J.; Edmeades, G.O. The Importance of the Anthesis-Silking Interval in Breeding for Drought Tolerance in Tropical Maize. *Field Crops Res.* **1996**, *48*, 65–80. [CrossRef]
70. Borrás, L.; Vitantonio-Mazzini, L.N. Maize reproductive development and kernel set under limited plant growth environments. *J. Exp. Bot.* **2018**, *69*, 3235–3243. [CrossRef] [PubMed]
71. Kim, H.C.; Moon, J.-C.; Kim, J.Y.; Song, K.; Kim, K.-H.; Lee, B.-M. Evaluation of Drought Tolerance using Anthesis-silking Interval in Maize. *Korean J. Crop Sci.* **2017**, *62*, 24–31. [CrossRef]
72. Byrne, P.F.; Bolaños, J.; Edmeades, G.O.; Eaton, D.L. Gains from Selection under Drought versus Multilocation Testing in Related Tropical Maize Populations. *Crop Sci.* **1995**, *35*, 63–69. [CrossRef]
73. Edmeades, G.O.; Bolanos, J.; Elings, A.; Ribaut, J.M.; Bänziger, M.; Westgate, M.E. The role and regulation of the anthesis-silking interval in maize. In *Physiology and Modeling Kernel Set in Maize*; CSSA Special Publications; Crop Science Society of America (CSSA): Madison, WI, USA, 2000; Volume 29, pp. 43–73. [CrossRef]
74. Monneveux, P.; Sanchez, C.; Tiessen, A. Future progress in drought tolerance in maize needs new secondary traits and cross combinations. *J. Agric. Sci.* **2008**, *146*, 287–300. [CrossRef]
75. Edmeades, G.O. Progress in achieving and delivering drought tolerance in maize–An update. In *Global Status of Commercialized Biotech/GM Crops*; The International Service for the Acquisition of Agri-biotech Applications (ISAAA): Ithaca, NY, USA, 2012.
76. Deressa, T.; Adugna, G.; Suresh, L.M.; Bekeko, Z.; Opoku, J.; Vaughan, M.; Prasanna, B.M. Biophysical factors and agronomic practices associated with Fusarium ear rot and fumonisin contamination of maize in multiple agroecosystems in Ethiopia. *Crop Sci.* **2024**, *64*, 827–884. [CrossRef]
77. Mesterhazy, A.; Szabo, B.; Szieberth, D.; Tóth, S.; Nagy, Z.; Meszlenyi, T.; Herczig, B.; Berenyi, A.; Tóth, B. Stability of Resistance of Maize to Ear Rots (*Fusarium graminearum*, *F. verticillioides* and *Aspergillus flavus*) and Their Resistance to Toxin Contamination and Conclusions for Variety Registración. *Toxins* **2024**, *16*, 390. [CrossRef]
78. Lana, F.D.; Paul, P.A.; Minyo, R.; Thomison, P.; Madden, L.V. Stability of Hybrid Maize Reaction to Gibberella Ear Rot and Deoxynivalenol Contamination of Grain. *Phytopathology* **2020**, *110*, 1908–1922. [CrossRef]